RSC Advances

This is an *Accepted Manuscript*, which has been through the Royal Society of Chemistry peer review process and has been accepted for publication.

Accepted Manuscripts are published online shortly after acceptance, before technical editing, formatting and proof reading. Using this free service, authors can make their results available to the community, in citable form, before we publish the edited article. This *Accepted Manuscript* will be replaced by the edited, formatted and paginated article as soon as this is available.

You can find more information about *Accepted Manuscripts* in the Information for Authors.

Please note that technical editing may introduce minor changes to the text and/or graphics, which may alter content. The journal's standard Terms & Conditions and the Ethical guidelines still apply. In no event shall the Royal Society of Chemistry be held responsible for any errors or omissions in this *Accepted Manuscript* or any consequences arising from the use of any information it contains.

ROYAL SOCIETY OF CHEMISTRY

www.rsc.org/advances

Cerium functionalized PVA-Chitosan composite nanofibers for effective remediation of ultra-low concentrations of Hg (II) in water

Reena Sharma [†], Nahar Singh[¥], Sangeeta Tiwari [†], Sandeep K. Tiwari[@], Sanjay R. Dhakate[¥ *]

[†] Amity Institute of Applied sciences, Amity University, Noida, 201303 (U.P., India)

[¥] CSIR-National Physical Laboratory, Dr. K.S. Krishnan Marg, New Delhi -110012, India

[@] Council of Scientific and Industrial Research, Rafi Marg, New Delhi-110001

Abstract

The contamination of mercury in drinking water significantly affects the human beings even at very low concentration and affecting the central nervous system, kidneys and other organs. Higher concentrations of mercury are reported to be effectively removed by adsorption and precipitation techniques. Reverse Osmosis (RO) is better known technique used for the removal of low concentration of Hg (<200 ppb). However, it has limitations of low flux, high water reject, high capital cost besides being power dependent. In present study reports the fabrication of low cost, biodegradable, electrospun Cerium functionalized PVA-Chitosan (Ce-PVA-CHT) composite nanofibers for effective removal of Hg (II) from water present in low concentrations. It adsorbs Hg (II) and purifies water up to safe potable limits as prescribed by WHO/US-EPA. The adsorption of Hg (II) over the surface of Ce- PVA- CHT is confirmed by SEM/ EDAX, FTIR, XRD and XPS techniques. The adsorption studies are reported by varying parameters viz. time, pH, adsorbent dose and varying contents of Ce in PVA-CHT nanofibers. Traceability is established by using SCP Science-UK make Certified Reference Standards for calibration of AAS-HG used for determination of Hg (II). The kinetic data shows fast and efficient removal of Hg (II) and indicates to follow pseudo second order kinetics. The adsorption data is best fitted to Langmuir isotherm and indicates monolayer adsorption of Hg (II).

Keywords: Ce-PVA-CHT composite nanofibers, Hg (II) adsorption, water purification, AAS-HG etc.

***Corresponding Author:**dhakate@mail.nplindia.org, Tel: 0911145608257, Fax: 091145609310

RSC Advances Accepted Manuscript

1. Introduction

Mercury (II) is a highly reactive ion which binds to the amino acid cysteine proteins. It is considered to be a carcinogen causing embryocidal, cytochemical, and histopathological events.[1] On converting into methyl mercury, mercury and its compounds can affect the human beings even at very low concentrations.[2, 3] The main sources for contamination of water by mercury are wastewater discharges from industries like chlor-alkali, paper and pulp, oil refining, paint, pharmaceuticals and batteries. United State-Environmental Protection Agency (US-EPA) has set a very low discharge limit for Hg in wastewater at 10 µg/L.[4] Various methods have been reported for removal of Hg (II) including chemical precipitation, ion exchange, membrane filtration, electrochemical separation, reverse osmosis, solvent extraction and adsorption.[5-7] Adsorption is considered to be a suitable option for it being fast and of low cost besides producing no sludge. Various non-conventional adsorbents have also been reported for Hg (II) remediation like fly ash, iron oxide-dispersed activated carbon fibers,[8] polymerized onion skin,[9] peat moss,[10] polymerized saw dust and cellulose.[11] Presence of nitrogen in Chitosan (CHT) is reported to show good affinity for Hg and other metallic elements. Therefore, nitrogen-rich polymers have been explored for Hg adsorption directly or as coating on adsorbents.[12, 13] CHT is considered as an excellent bio adsorbent for removal of cations of metallic element at near-neutral pH owing to presence of large number of amino groups. Hydrophilicity, presence of large number of functional groups, high chemical reactivity, flexible polymer chains and biodegradability makes CHT a material of choice for adsorption of metallic elements.[14] The cationic behavior of CHT facilitates attraction of metal anions due to the protonation of amino groups in acidic medium.[15] Composites of CHT have been reported for removal of heavy metals. Chitin/cellulose composite membranes are reported for effective removal of Hg (II).[16] Chitosan as modified magnetic chitosan,[17] chitosan-coated magnetite nanoparticles,[18] thiol grafted chitosan,[19] aminated chitosan beads,[20] chitosan and chitosan derivatives grafted with poylacrylamide [21] are reported as effective adsorbents for Hg (II). However, removal of Hg (II) at low concentrations is a challenging task. The literature indicates that most of the adsorbents require longer exposure time for effective removal. The present study attempts to remove the drawbacks associated with adsorbents reported earlier, by fabricating PVA-CHT composite nanofibers functionalized with Ce, for efficient removal of Hg (II) from water present in low concentrations.

RSC Advances Accepted Manuscript

2. Experimental

2.1 Materials and apparatus:

Chitosan powder (M.W; 100000-300000) from Across Organic, Polyvinyl-alcohol (M.W: approx. 125000) from CDH, formic acid, Cerium (III) nitrate hexahydrate (M.W: 434.23) from Chemica-biochemica reagents, Sodium borohydride ($NaBH_4$), Hydrochloric acid (HCl), Ammonium hydroxide (NH_4OH), Potassium hydroxide (KOH), Nitric acid (HNO_3), and Potassium nitrate (KNO_3) from E. Merck India were used. Double distilled water was employed for all the synthesis work while deionized water (DI) of 18.2 mega Ω resistivity (Millipore, USA) was used for preparing samples for AAS-HG analysis.

Electro Spinning Equipment (Physics Instrument Company, Chennai, India) was used to synthesize Ce-PVA-CHT composite nanofibers. The surface morphology and elemental distribution in Ce-PVA-CHT composite nanofibers was determined by Scanning Electron Microscope (SEM) (Model EVO M-1; Ziess), attached with Energy Dispersive X-ray Spectroscopy (EDAX) for measuring elemental composition. Fourier Transform Spectrophotometer (FTIR) (Model Nexus-47; Nicolet) was used to analyze functional groups, while X-ray Diffraction (XRD) patterns of composite nanofibers were recorded on Expert D6 model, Japan (λ-1.5404 Å). The un-adsorbed concentration of Hg (II) was determined on AAS-HG (Vario-6-Analytik Jena, Germany). The adsorption studies for Hg (II) removal was carried out using reference standards (SCP Science, USA) after appropriate dilutions. X-ray Photoelectron Spectroscopy (XPS) spectra were recorded on MULTILAB 2000 (Thermo Scientific, USA) using an X-ray (Mg Kα radiation source) with a binding energy scan range of 0-1200 eV and the work function of the spectrometer was 4.1 ± 0.1 eV. The collected high resolution XPS spectra were analyzed using an XPS peak fitting software program.

2.2 Fabrication of Ce-PVA-CHT composite nanofibers:

Ce-PVA-CHT composite nanofibers were prepared by Electro Spinning technique[22] after optimizing the processing parameters. It has been observed, from the various combinations of PVA and CHT ratio, bead free nanofibers were obtained at 7:3 ratio of PVA: CHT. Therefore, homogenous solutions of CHT powder (4 wt %) in 2% (v/v) formic acid and PVA (8 wt %) in 2% (v/v) acetic acid were prepared under magnetic stirring at room temperature. PVA and CHT solutions were mixed together in 7:3 ratios by magnetic stirrer for 4-5 hr to get a solution of

RSC Advances Accepted Manuscript

desirable viscosity. Cerium (III) nitrate hexa-hydrate (0.5-5.0 w/ w %) was then added and mixed until clear solution was obtained. This solution was used for electro spinning using 2 mL syringe at 20 kV with flow rate of 0.2 ml/h. A distance of 18-20 cm was maintained between syringe tip and collector. Aluminum foil was wrapped on rotating collector to collect the composite nanofibers. Ce-PVA-CHT composite nanofibers were cured at ~110°C for 5 hours prior to its use for Hg (II) adsorption studies.

2.3 pH_{PZC} determination:

The pH_{pzc} determination of Ce-PVA-CHT composite nanofibers was carried out by the method reported earlier.[23] The composite nanofibers were suspended in 25 mL of 0.03 M KNO_3 solution and kept overnight to stabilize the pH with continuous stirring followed by the addition of 0.1 mL of 1M KOH. The pH value of above solution was recorded after each addition of 0.1 M HNO_3. Blank titration with 0.03 M KNO_3 was also carried out following the same process to get the potentiometric curve between pH and volume of HNO_3 consumed. The intersection point in potentiometric curve (Fig. 8a) was considered as pH_{pzc} of Ce-PVA-CHT composite nanofibers.

2.4 Adsorption studies:

The batch adsorption studies were conducted by suspending composite nanofibers in Hg (II) solution. The stock solution of Hg (II) was diluted to desirable concentrations for studies and pH was adjusted with the help of dilute Hydrochloric acid or Ammonium hydroxide solutions. Thus, adsorbent was suspended in 100 ml of Hg (II) in beaker and stirred for 75 minutes on magnetic stirrer (~50 rpm; ambient temperature). After removing the adsorbent from the solution, the analyte concentration in the remnant was determined by AAS-HG.[24, 25]

The adsorption capacity (q_e) and efficiency were calculated by using following equations:

$$\text{Adsorption capacity } (q_e) = \frac{(C_i - C_f) * V}{m} \quad \text{------ (1)}$$

$$\% \text{ Removal} = \frac{(C_i - C_f) * 100}{C_i} \quad \text{------ (2)}$$

Where, 'C_i' and 'C_f' (mg/L) are the initial and final concentration of Hg (II) solution, respectively; V is the volume (L) of the solution and 'm' is the weight (g) of Ce-PVA-CHT composite nanofibers.

RSC Advances Accepted Manuscript

A series of adsorption experiment were conducted by varying conditions like pH, adsorbent dose and Ce content in Ce-PVA-CHT composite nanofibers for adsorption of Hg (II). Kinetics and equilibrium studies were conducted for Langmuir and Freundlich isotherms at optimized conditions with varying concentrations (0.1-20 mg/L) of Hg (II).

Recyclability and reuse of Ce-PVA-CHT composite nanofibers used in Hg (II) adsorption was ascertained.[26] Three cycles of regeneration were carried out by treating Hg loaded Ce-PVA-CHT nanofibers with 0.01 M HCl. Thus, 15 mg of adsorbent was suspended in 100 ml of Hg (II) of 1000 (μg/L) and was continuously stirred on magnetic stirrer for 75 min at ~50 rpm. After determining the concentration of Hg (II) in the remnant solution, the Hg-loaded adsorbent was treated with 50 ml solution 0.1M HCl followed by thorough rinsing with DI water. The regenerated adsorbent was subjected to 2nd and 3rd cycle of adsorption.

3.0 Results and Discussion:

3.1 SEM and EDAX

CHT is de-acetylated polymer of chitin which is soluble in most of the acids as it gets protonated in acidic medium.[27] Neat CHT solutions in acids are difficult to electrospun due its higher viscosity [28], whereas PVA solutions can be easily electrospun[29]. For optimizing the solution parameters, different weight ratios of PVA and CHT (1-9:9-1) were investigated in the present course of work. Among the different experiment, it is observed that beads free nanofibers are obtained at 7:3 weight ratio of PVA and CHT. This was ascertained by SEM observations. Therefore, to produce functionalized composite nanofibers, in PVA and CHT solution prepared from in 7:3 weight ratio PVA and CHT, Cerium (III) nitrate hexahydrate (0.5-5.0 %) was added to get composite solution. While optimizing Ce content in PVA-CHT composite nanofibers, it was observed that Ce content between 0.5- 3.5% produces continuous and bead free nanofibers, whereas Ce content >3.5% produces beaded, discontinuous nanofibers having droplets. On the basis of these observations, composite nanofibers with Ce content of 3.5% were prepared for adsorption studies.

SEM images and EDAX of Ce-PVA-CHT composite nanofibers, before and after adsorption are depicted in the Fig. 1(a&b). Fig.1 (a) shows the nanofibers having mat like structure with smooth morphology without any beads but there is some variation in nanofibers diameter. The elemental analysis by EDAX of composite nanofibers before adsorption shows the presence of C, Ce, and

RSC Advances Accepted Manuscript

O only. There is change in surface morphology of Ce-PVA-CHT composite nanofibers after adsorption, demonstrated in Fig. 1(b). The composite nanofibers appear to have swollen after exposure possibly due to the absorption of water as a consequence hydrophilic nature PVA polymer. EDAX analysis of the composite matrix after adsorption (Fig. 1(b)) establishes the presence Hg (II) along with Ce, C, and O.

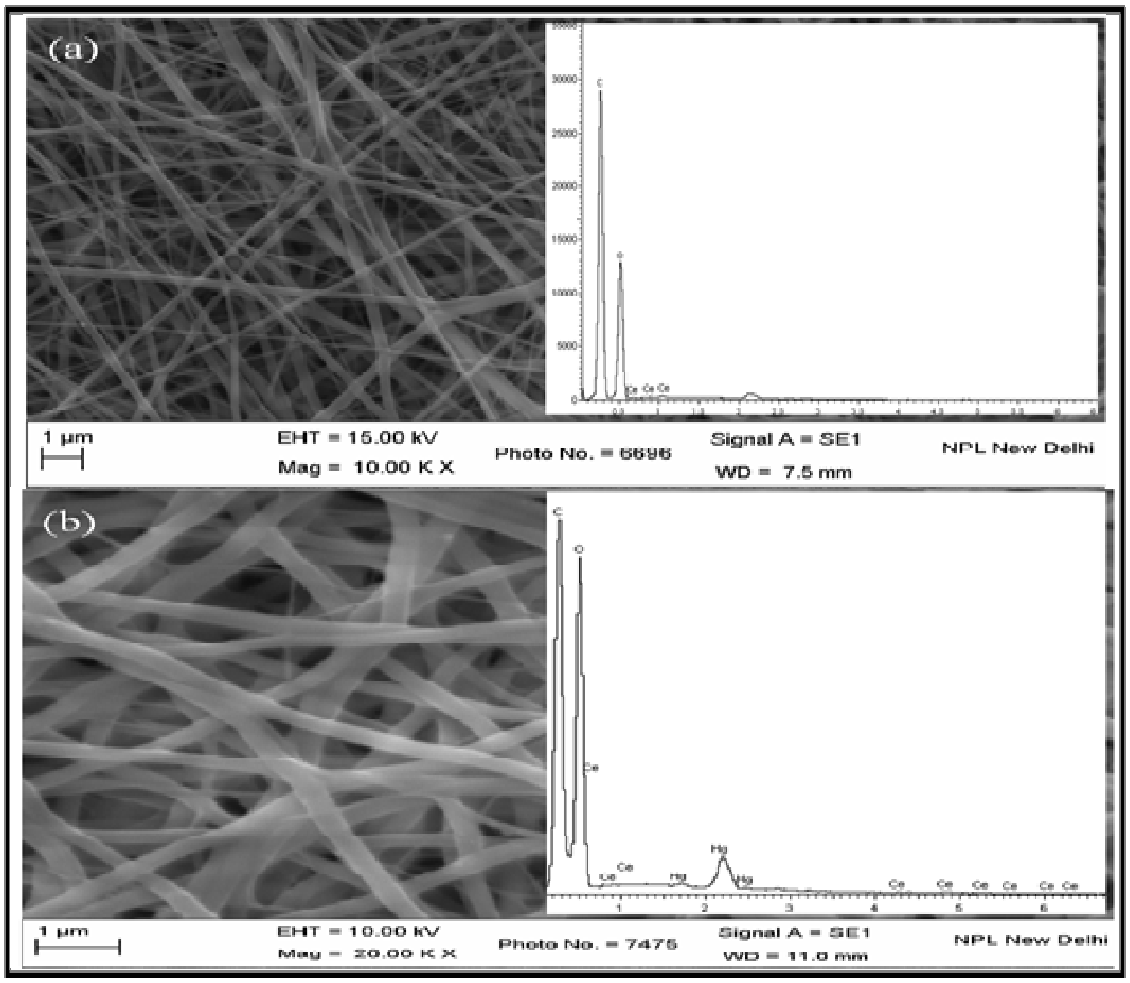

Figure1: SEM and EDAX of Ce-PVA-CHT composites nanofibers **(a)** Before adsorption, (**b)** After adsorption of Hg (II)

The elemental mapping of Ce-PVA-CHT composite nanofibers shown in Fig.2 illustrates uniform distribution of adsorbed Hg (II) on the surface of composite nanofibers.

RSC Advances Accepted Manuscript

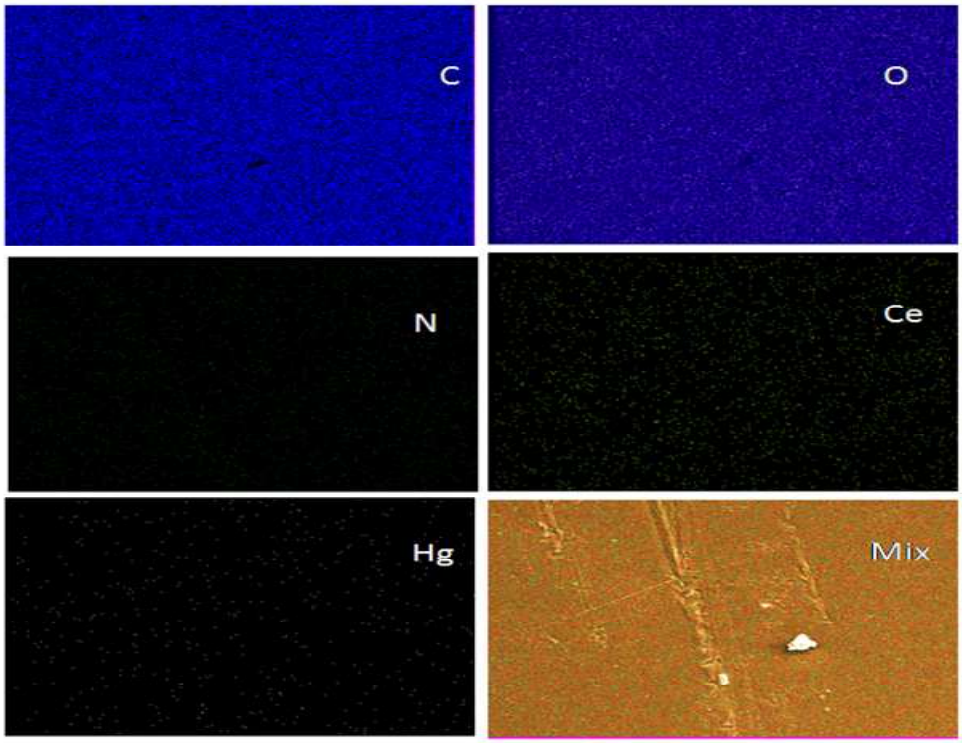

Figure 2: Elemental (C, O, N, Ce & Hg) mapping Ce-PVA-CHT composite nanofibers after adsorption of Hg (II)

3.2 FTIR studies:

Fig.3 (a, b & c) illustrates FTIR spectra of PVA-CHT, Ce-PVA-CHT composite nanofibers with and without Hg (II), respectively.

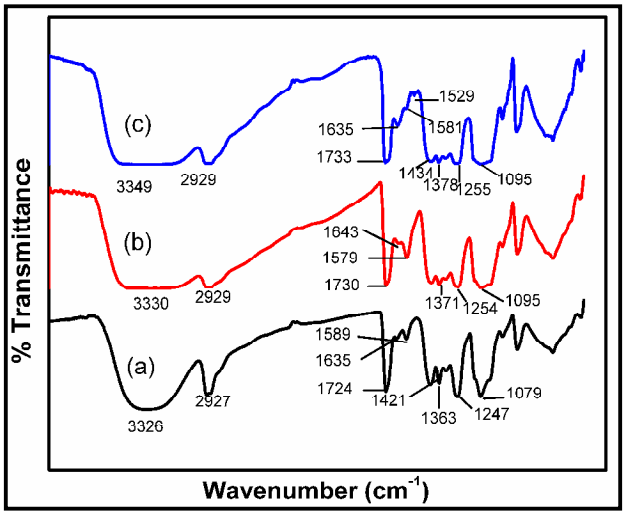

Figure 3: FTIR of (a) PVA-CHT, (b) Ce-PVA-CHT, and (c) Ce-PVA-CHT composite nanofibers after adsorption of Hg (II)

RSC Advances Accepted Manuscript

The spectrum of PVA-CHT nanofibers (Fig. 3(a)) shows the broad adsorption band at ~ 3326 cm^{-1} indicating -OH stretching of water and overlapping of -NH bands of CHT. The absorption band with maxima at 1724 cm^{-1} shows presence of O=C-NH group in PVA/CHT composite nanofibers, while the absorption at 1635 cm^{-1}, 1589 cm^{-1} and 1363 cm^{-1} indicate presence of amide groups- a characteristic of CHT.[30] Bands with maxima at 1079 cm^{-1} and 1421 cm^{-1} are the stretching vibrations of C=O and -OH in PVA, respectively. Interaction of -NH group in CHT with Ce may be responsible for shifting of adsorption peaks at 1363 cm^{-1} and 1075 cm^{-1} in (Fig 3(a)) to 1371 cm^{-1} and 1095 cm^{-1} (Fig. 3(b)), respectively.[15] The C-H stretching vibrations are seen at 2929 cm^{-1} in each curve.[31] While peaks at 1643 cm^{-1} and 1579 cm^{-1} show shifts, the intensity of peak at 1581 cm^{-1} is observed to increase (Fig. 3(b) &(c)). The shifting of absorption peaks at 1643 cm^{-1} and 1579 cm^{-1} (Fig. 3(b)) towards the 1635 cm^{-1} and 1581 cm^{-1} along with formation of new peak at 1529 cm^{-1} (Fig. 3(c)), may be attributed to coordination of Hg (II) with nitrogen present in composite nanofibers.[17] Therefore, it can be concluded that –NH groups in CHT are mainly responsible for the interaction of Hg (II) on Ce-PVA-CHT composite nanofibers. The shifting of 3330 cm^{-1} to 3349 cm^{-1} also indicates the binding of Hg (II) with oxygen atom of hydroxyl groups as adsorption site for Hg (II) removal.[17] Earlier studies suggest that -NH_2 and -OH groups of chitosan are also involved in adsorption of other metals like Co, Pb and Cr.[32-34]

3.3 XRD:

The XRD patterns are illustrated to examine the adsorption behavior of Hg (II) over the surface of Ce-PVA-CHT composite nanofibers. The XRD pattern of CHT exhibits diffraction peaks at 2θ = 10.5º, 15.4 ° and 20.1º indicating formation of semi-crystalline structure of CHT.[35] Diffraction peaks at 2θ= 10.7 º and 20.4 º show inter and intra molecular hydrogen bonding in PVA.[36] XRD patterns given in Fig. 4 (a) & (b) show appearance of two peaks at 2θ= 9.16° and 19.32° while peak at 15.4° disappears indicating interaction of PVA with CHT which results in less crystalline structure of CHT. Diffraction peaks at around 38° and 44° are due to Ce complexation with PVA-CHT. However, after adsorption of Hg (II) on composite nanofibers the peaks at 9.16 ° and 19.32° in Fig. 4(a) show shift towards 2θ= 9.3° and 19.9° with increase in intensity (Fig.4(b)) indicating adsorption of Hg (II) on Ce-PVA-CHT composite nanofibers with

RSC Advances Accepted Manuscript

increased crystallinity. The 2θ value 9.16° and 19.32° are related peaks of CHT which indicates the interaction of Hg (II) with nitrogen present in it.

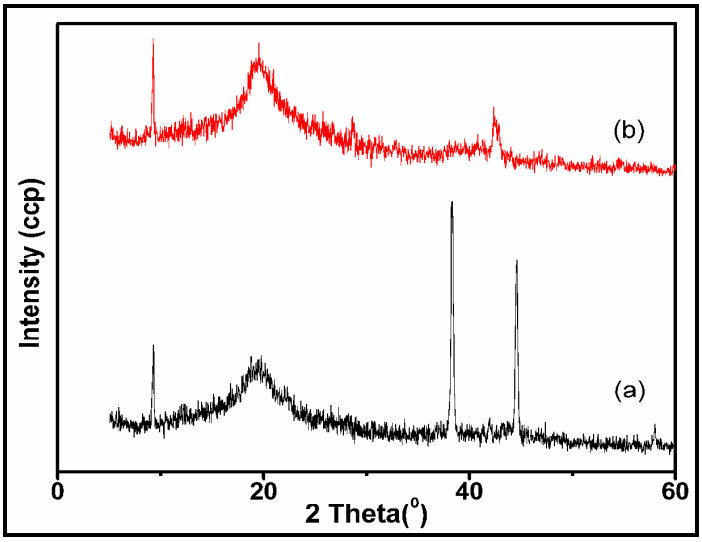

Figure 4: XRD of Ce-PVA-CHT composite nanofibers (a) before and (b) after adsorption of Hg (II)

3.4 X-ray Photon Spectroscopy (XPS):

The interaction of Hg (II) with the surface of Ce-PVA-CHT composite nanofibers was studied by XPS. Wide scan survey of Ce-PVA-CHT composite nanofibers before and after adsorption has been illustrated in Fig. 5. The spectrum is showing two C1s peaks for adsorbed composite sample (Fig. 5(b)) having binding energy 284.9 and 289.5 eV. A doublet is also seen for O1s peak having binding energies of 533.0 and 538.1 eV. These peaks could be assigned for presence of - OH, - O -, and C=O in composite nanofibers. Some other oxygen contamination forms such as C=O and O—H of water might be associated besides this there is a possibility for oxygen contamination as a result of the reaction with the atmospheric oxygen when the composite nanofibers were exposed to air. The peak area between 850 to 895 eV belongs to the Ce 3d5/2. Doublet at 101 eV (Hg $4f_{5/2}$) and 104.5 eV (Hg $4f_{7/2}$) associated with Hg (II) [37, 38] is not well resolved due to contamination and significant noise in Hg 4f region of XPS spectra. Since EDAX and elemental mapping indicates adsorbed Hg (II), the appearance of peak at 102.5 eV can be considered as Hg 4f peak for oxidized mercury (Hg (II).

RSC Advances Accepted Manuscript

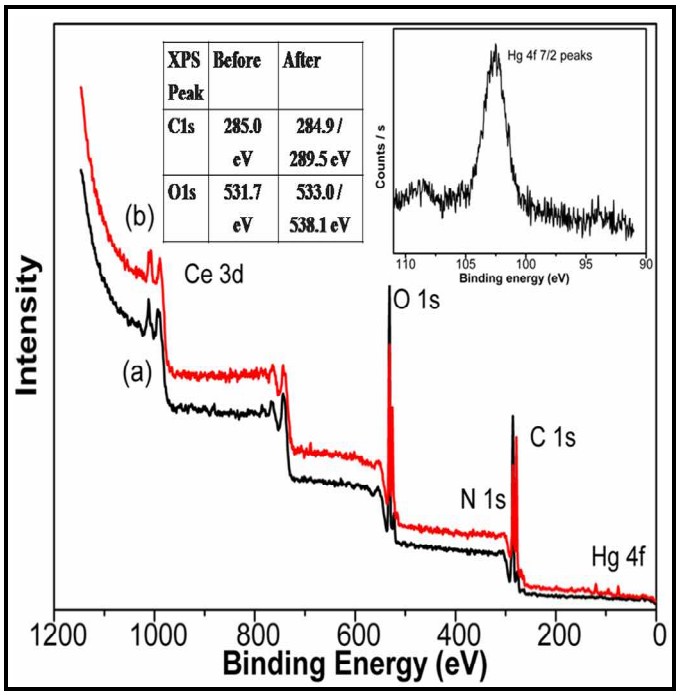

Fig. 5: XPS of Ce-PVA-CHT composite nanofibers before and after adsorption of Hg (II)

3.5: Adsorption Kinetics

The efficiency of Hg (II) adsorption with time is carried out by exposing Ce-PVA-CHT composite nanofibers (15 mg) in solution of Hg (II) (5.0 mg/L) (pH: 5.3-6) at ambient temperature. Fig. 6 (a) shows rapid adsorption of Hg (II) at initial stages indicating availability of more active site for interaction. However, with passage of time, the adsorption decreases. The equilibrium is reached after 75 min indicating that the composite nanofibers have reached the maximum adsorption capacity. To understand the characteristics of adsorption of Hg (II), Pseudo first order (3) and pseudo second order (4) model were applied to fit the experimental data of batch studies. [39-42]

$$\ln (q_e - q_t) = \ln q_e - k_1 t \quad \text{------ (3)}$$

$$\frac{t}{q_t} = \frac{1}{k_2 q_e^2} + \frac{t}{q_e} \quad \text{------ (4)}$$

If time‘t’ is zero then the initial sorption rate ‘h’ becomes:

------ (5)

RSC Advances Accepted Manuscript

$$h = k_2 q_e^2$$

Where 'q_e' and 'q_t' (mg/g) represents the adsorption capacities at equilibrium and at time't', respectively; 'h' (mg/g*min) is the initial adsorption rate and 'k' (g/mg *min) is the rate constant.

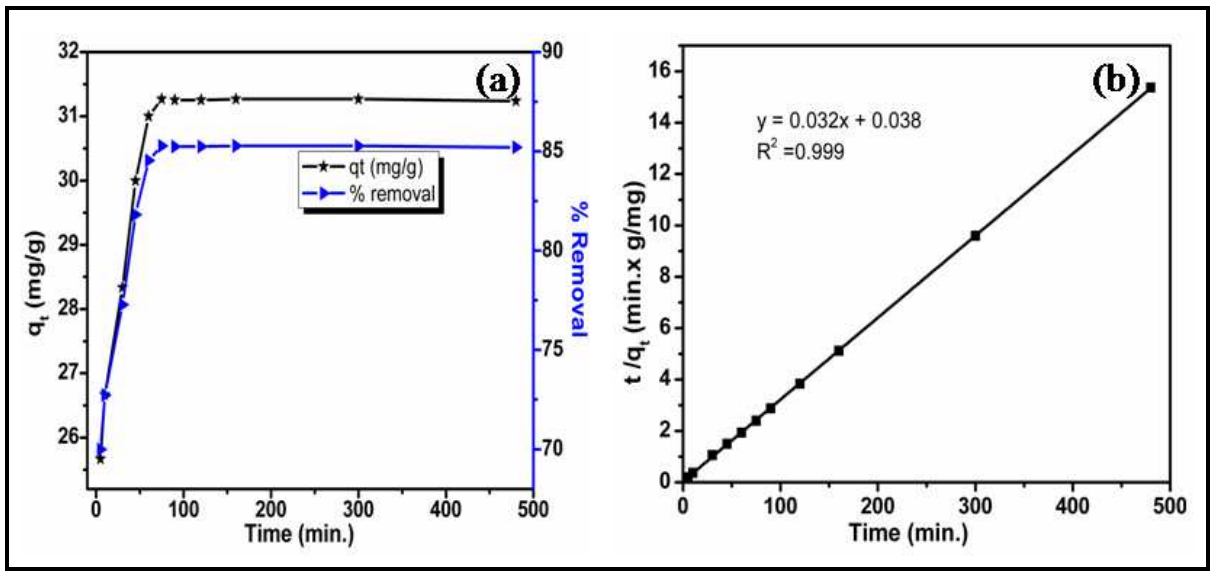

Figure 7:(a) Effect of contact time on adsorption capacity (q_e) of Hg (II), (b) Pseudo second order kinetics

Fig.6 (a) shows effect of time on adsorption capacity while Fig. 6 (b) illustrates pseudo second order kinetic model. The adsorption capacity (q_e), rate constant (k) and coefficient of determination (R^2) has been obtained from Fig. 6 (b). The values of 'q_e', 'k' and 'R^2' calculated from slope and intercept are 31.25 mg/g, 0.03 g/mg. min and 0.999, respectively. Fig.7 shows pseudo first order kinetics which indicates poor fit to data with k_1 =0.0121 (min.$^{-1}$) obtained from the plot of ln (q_e-q_t) versus t. However the experimental data deviates from calculated data in case of pseudo first order model and also correlation coefficients, R^2 = (0.826) is less than pseudo second order R^2 (0.999). These findings suggest that adsorption data does not follow pseudo first order kinetics. The q_e obtained from pseudo second order plot is very close to the experimental q_e (31.26 mg/g) and the correlation coefficient also exceeds 0.999. These results indicate that pseudo second order model closely fits to the data of Hg (II) adsorption. Other studies[43, 44] indicates, pseudo second order model gives better results using type-1 equation among other liberalized form of pseudo second order equations.

RSC Advances Accepted Manuscript

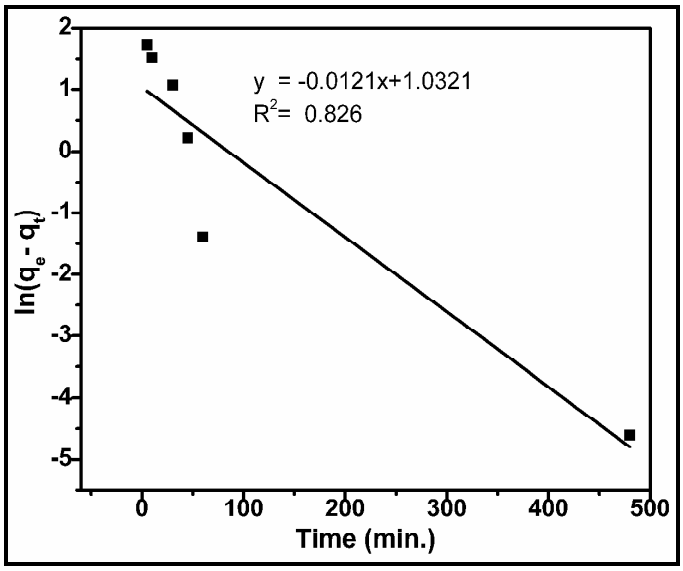

Figure 7: Pseudo first order kinetic

3.6 Influence of pH, dose and Ce content on Hg (II) adsorption:

The pH plays an important role in adsorption process for Hg (II) as it controls the surface charge of the adsorbent and the degree of ionization of adsorbate in aqueous solution and facilitates the solid and liquid interface during the adsorption process. The adsorption behavior of Ce-PVA-CHT as a function of pH was examined by exposing 15 mg nanofibers in 100 ml of Hg solution (5.0 mg/L) at different pH (2-10) (Fig. 8 (b)). Adsorption of Hg (II) increases continuously from pH 2 to 5 while at pH (5.3 to 6.0), the adsorption of Hg (II) stabilizes. At higher pH (>6.0) the adsorption of Hg (II) decreases gradually. Formation of metal hydroxide species like soluble Hg(OH)+ or insoluble precipitate of $Hg(OH)_2$ could be the reason.[45] The pH_{PZC} of Ce-PVA-CHT composite nanofibers (Fig.8 (a)) was found in the range of 6.6-7.3. This is very close to the reported pH_{PZC} of CHT i.e. (6.4-7.2).[46] The occurrence of adsorption at near neutral pH indicates interaction of amino groups of composite nanofibers with Hg (II). The free lone pair of electrons on nitrogen atom of CHT participates in coordination with the metal ion to give the corresponding CHT–metal complex. It has also been reported that at pH 5-6, the presence of amino group in CHT (pK_a = 6.5) gets protonated and H^+ ions are produced in the presence of HCl which leads to formation of anion complexes, such as $HgCl_3^-$.[1] This anion is adsorbed on Ce-PVA-CHT composite nanofibers [18, 47] by complex formation with amino and Ce present in

RSC Advances Accepted Manuscript

composite nanofibers. No significant change in pH value of solution before and after Hg (II) adsorption was observed.

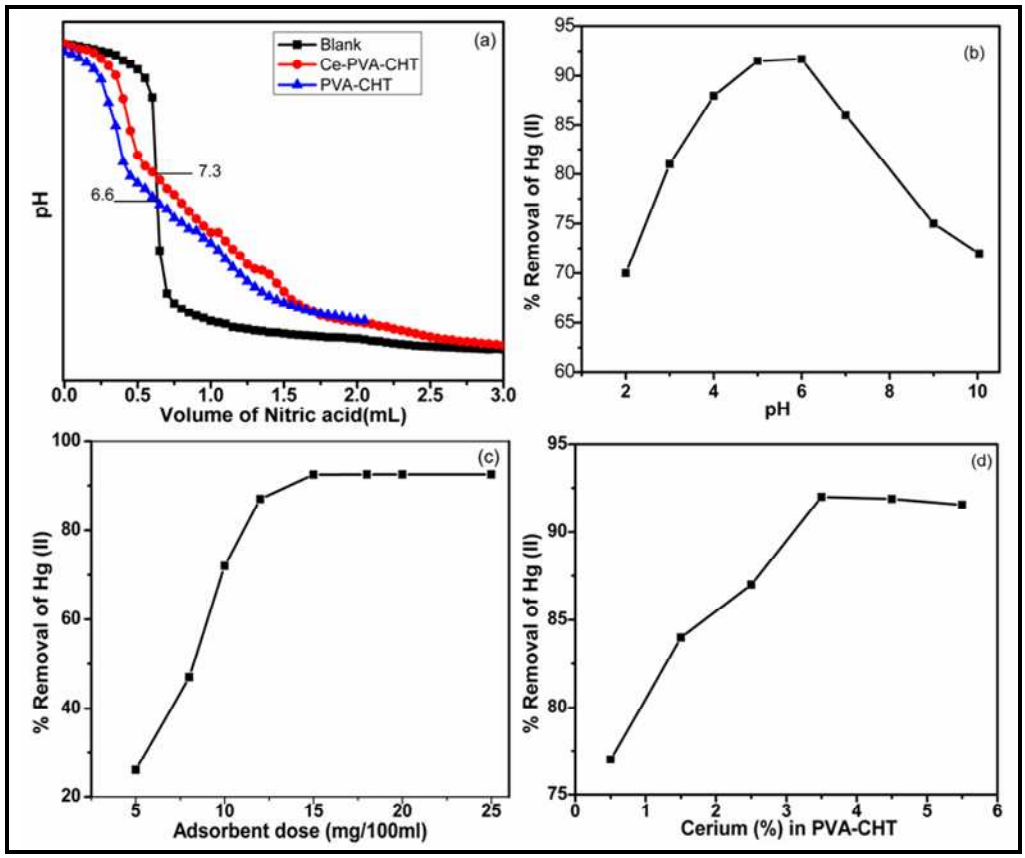

Figure 8: (a) pH_{PZC} (b) Effect of pH, (c) Effect of dose and (d) Effect of Ce content in PVA-CHT Hg (II)adsorption

The influence of adsorbent dose on the adsorption of Hg (II) is carried out in 100 mL of 5.0 (mg/L) Hg (II) solutions. The adsorbent dose is varied from 5 to 20 mg. Fig. 8 (c) shows the increase in % removal of Hg (II) with increased adsorbent dose. The observation indicates the increase in availability of free sites to bind Hg (II). With further increase in dose after achieving the maximum removal at 15 mg/100ml, no increase in adsorption is observed. This indicates that some amount of Hg (II) ions remain in solution even after further addition of adsorbent dose.

Adsorption of Hg (II) as a function of Ce content in PVA-CHT is illustrated in Fig. 8 (d). Adsorption of Hg (II) increases on increasing Ce content from 0.5-3.5 % in PVA-CHT blend. The nanofibers with 3.5 % of Ce content show the maximum adsorption. The higher concentration of Ce makes the solution more viscous resulting in the formation of beaded and

RSC Advances Accepted Manuscript

non-uniform nanofibers and therefore nanofibers with higher concentration of Ce are not prepared.

3.7Adsorption Isotherms:

Adsorption isotherms are useful tool to understand the adsorption process like the equilibrium relationship between the solid and liquid interface. Adsorption isotherms can be expressed in the form of Langmuir, Freundlich, Temkin and Dubinin-Radushkevich.[48] Langmuir and Freundlich isotherms are most commonly used adsorption isotherm models. Langmuir isotherm which describes the adsorption of adsorbate onto the surface of the adsorbent is based on following assumptions: The adsorbent's surface is in contact with a solution having adsorbate attracted to the surface. Adsorbent surface has a specific number of active sites to bind solute's molecules. Only monolayer adsorption occurs on the surface of adsorbent. Whereas Freundlich isotherm commonly describes the adsorption characteristics for the heterogeneous surface or shows multilayer's adsorption of adsorbate onto the surface of adsorbent.[49]

To investigate the effect of concentration of metal ions on adsorption, the batch adsorption studies are carried out by exposing 15 mg of Ce-PVA-CHT composite nanofibers in 100 ml of Hg (II) solution under constant stirring for 75 min. The ion concentrations are varied from 0.1 to 20 mg/L. After adsorption, the concentration 'C_f' of Hg (II) in solution is measured by AAS-HG. Results depicted in Fig. 9 (a&b) indicate increases in Hg (II) adsorption capacity with increase in concentration of Hg (II) while showing decrease in adsorption in percentage terms. It is observed (Fig.9 (a)) that composite nanofibers effectively remove Hg (II) from 1000 µg/L to the levels specified by WHO /US-EPA. It is also effective in removing even lower (<200 µg/L) concentrations of Hg (II). Highest adsorption 'q_m' occurs at Hg (II) concentration of 5000 µg/L. Additional adsorption of Hg (II) is not observed after further increase in concentration of metal ion. Saturation of all active sites of adsorbent with Hg (II) on the surface of adsorbent would be the reason. The experimental data obtained from batch studies were applied to the Langmuir (6) and Freundlich (7) isotherms:

$$\frac{C_f}{q_e} = \frac{1}{K_L\, q_m} + \frac{C_f}{q_m} \qquad \text{----- (6)}$$

$$q_e = K_f . C_f^{\,1/n} \qquad \text{----- (7)}$$

RSC Advances Accepted Manuscript

Where, 'q_m' and 'q_e' in mg/g is the maximum adsorption capacity and adsorption capacity at equilibrium, respectively; 'C_f' in mg/L is the final concentration of Hg (II) solution after adsorption; and K_L in L/mg is the energy of reaction. The value of 'q_m' and 'K_L' are determined from slope and intercept of Fig. 9 (b). The valve of 'q_m', 'K_L' and 'R^2' are found to be 31.44 mg/g, 0.035 L/mg and 0.999, respectively. The experimental data is well fitted to Langmuir isotherm which suggests monolayer adsorption over the surface of Ce-PVA-CHT composite nanofibers.

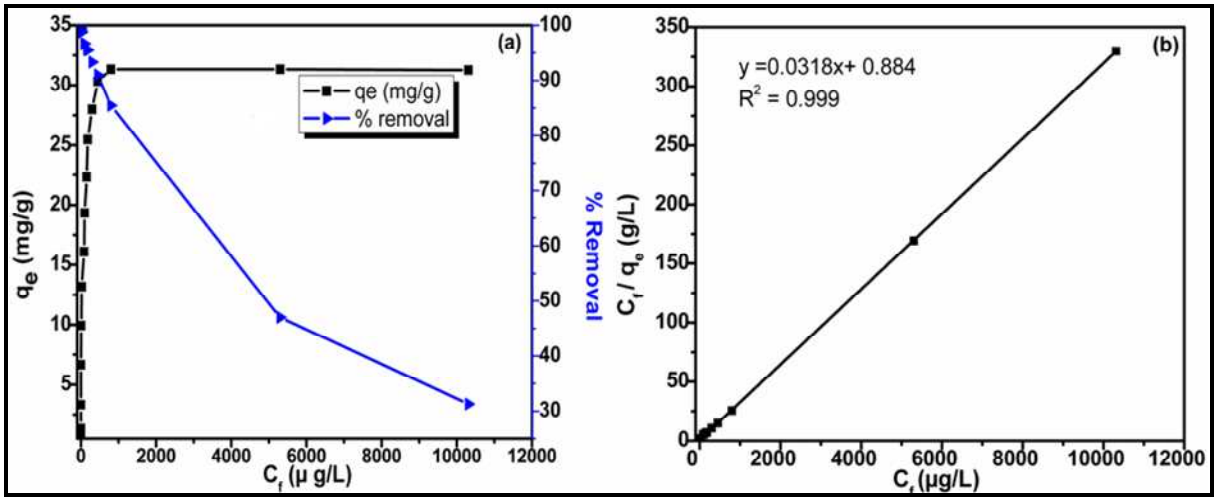

Figure 9: (a) Effect of initial concentration of Hg (II) on adsorption and (b) Langmuir adsorption isotherm

Langmuir isotherm can also be expressed by a dimensionless constant; the equilibrium parameter 'R_L' (separation factor) which is very useful in predicting feasibility and shape of the isotherm of the adsorption process by equation:

$$R_L = \frac{1}{1 + 1\,(K_L C_i)} \qquad \text{----- (7)}$$

Where: 'K_L' is related to energy of adsorption called as Langmuir Constant. On the basis of 'R_L', nature of adsorption of Hg (II) over Ce-PVA-CHT composite nanofibers can be predicted as unfavorable (>1), linear (=1), favorable (>0 or <1) or irreversible (=0). In the present

RSC Advances Accepted Manuscript

investigation 'R_L' value lies between zero and one i.e. (>0 or <1) indicating that adsorption of Hg (II) over Ce-PVA-CHT composite nanofibers is favorable.

The eq. (6) can also be represented as:

$$\log q_e = \log K_f + 1/n \log C_f \quad \text{----- (8)}$$

The plot of 'log q_e' Vs 'log C_i' represents the applicability of Fruendlich isotherm. The Freundlich isotherm is based on the assumption that adsorption occurs at the heterogeneous surfaces and any foreign material or pollutant can be allowed to adsorb in multilayer of an adsorbent.[50]

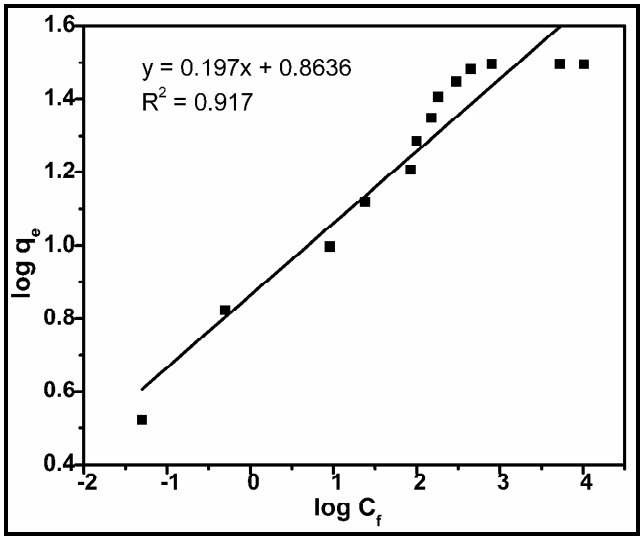

Figure 10: Freundlich Isotherms

Fruendlich constants 'K_f' (L/g) and 'n' are related to adsorption capacity and adsorption intensity, respectively. The values are calculated from slope and intercept of Fig. 10. It also explains the dependence of adsorption on initial concentration of Hg (II). If (1/n) < l, the bond energies increases with the surface density; if (1/n) > l, the bond energies decreases with the surface density and when n = 0, all surface sites are equivalent. The calculated value of n (=1.57 from Fig.10) indicates favorable adsorption. It may be noted that if 1/n value is below 1,

RSC Advances Accepted Manuscript

adsorption follows the Langmuir isotherm whereas if the value of 1/n is greater than 1, cooperative adsorption occurs.

3.8 Removal of Hg (II) in presence of diverse ions:

Ce-PVA-CHT composite nanofibers effectively remove Hg (II) from 1000 ppb to safe potability limits prescribed by WHO/US-EPA. The experiments are carried out using municipal tap water spiked with known concentration of Hg (II). The tap water contains Na, Ca up to 1000 ppm, K, Mg up to 150 ppm, Fe 2.5 ppm, chloride 30.5 ppm and TDS 550 ppm. It is observed that more than 99.0% of Hg (II) is effectively removed from the sample prepared in tap water. Individual effects of ions were also examined and it is found that Na, Ca, K and Mg do not interfere significantly. However, presence of Fe and Cl ions in water decreases the adsorption of Hg (II) up to 10%. Other metal ions like Zn, Pb, Cu, Ni, Cd and Mn also affects the adsorption on composite nanofibers and significantly interferes in Hg (II) removal (Table-1).

Table -1: Removal of Hg (II) in presence of other metal ions

S.N.	Species	Hg (µg/L)	Added species (µg/L)	Hg (µg/L) left in solution
1.	Hg(II)	1000	0.00	0.53
2.	Zn	1000	200	25.3
3.	Pb	1000	200	6.5
4.	Cu	1000	200	2.8
5.	Ni	1000	200	6.8
6.	Cd	1000	200	29.3
7.	Mn	1000	200	11.2

Recycling /regeneration of Ce-PVA-CHT:

For ascertaining reusability, the Hg adsorbed composite nanofibers are subjected to regeneration by treating with 0.01M HCl followed by thorough washing with DI water and drying. The Ce-PVA-CHT used in first cycle shows removal of almost 1000 µg/L of Hg (II) whereas 68% and 38% is removed in 2nd and 3rd cycle. Mild acidic conditions used for regeneration coupled with

RSC Advances Accepted Manuscript

susceptibility of Ce-PVA-CHT to acidic medium could be responsible for reduced adsorption after successive cycles. The SEM examination indicates deterioration of morphology of regenerated nanofibers to little bit rough than neat nanofibers because of surface etching by HCl. After 3rd cycle, the adsorption capacity of nanofibers is significantly reduced. This could be due to significant stripping of CHT from the nanofibers or ineffective removal of Hg (II) during its regeneration under mild acidic conditions.

4. Conclusions

A low cost, nontoxic, biodegradable Ce-PVA-CHT composite nanofiber mat has been fabricated by electrospinng technique for efficient removal of Hg (II). SEM-EDAX, FTIR, XRD and XPS studies confirm the adsorption of Hg (II) on Ce-PVA-CHT composite nanofibers. Functionalization of PVA-CHT by Ce is observed to improve the adsorption behavior as small ionic radii, high electric charge and high potential energy of Ce helps in increasing the adsorption of Hg (II) on composite nanofibers. The maximum efficiency (31.44 mg/g) for Hg (II) removal was observed at 3.5% Ce content in PVA-CHT composite nanofibers. Ce-PVA-CHT best works in pH range of 5.3-6.0. The kinetics of adsorption process indicates fast and efficient removal of Hg (II) while conforming to pseudo second order kinetics model. The Langmuir isotherm shows monolayer adsorption. The fabricated composite nanofibers effectively remove Hg (II) at low to moderate concentrations. The adsorption studies, carried out on municipal tap water containing several ionic species, shows composite to efficiently remove Hg to safe potable water limits of WHO/US-EPA. Considering the nonwoven structure, its capacity to remove Hg (II) rapidly and even at low concentrations, the reported composite nanofibers could be potential alternative for fast (high flux) and effective removal of Hg (II) from contaminated water.

References:

1. P. Miretzky and A. F. Cirelli, *Journal of hazardous materials*, 2009, 167, 10-23.
2. J. G. Dorea and C. M. Donangelo, *Clinical nutrition*, 2006, 25, 369-376.
3. E. M. Nolan and S. J. Lippard, *Chemical reviews*, 2008, 108, 3443-3480.
4. K. H. Nam, S. Gomez-Salazar and L. L. Tavlarides, *Industrial & engineering chemistry research*, 2003, 42, 1955-1964.
5. M. Monier, D. Ayad, Y. Wei and A. Sarhan, *Reactive and Functional Polymers*, 2010, 70, 257-266.

RSC Advances Accepted Manuscript

6. F.-C. Wu, R.-L. Tseng and R.-S. Juang, *Water Research*, 2001, 35, 613-618.
7. F. Pérez-García, C. A. Galán-Vidal, J. G. Alvarado-Rodríguez, M. E. Páez-Hernández, N. Andrade-López and M. T. Ramírez Silva, *Separation Science and Technology*, 2013, 48, 736-740.
8. W. Knocke and L. Hemphill, *Water research*, 1981, 15, 275-282.
9. P. Kumar and S. Dara, *Journal of Polymer Science: Polymer Chemistry Edition*, 1981, 19, 397-402.
10. P. Brown, S. Gill and S. Allen, *Water Research*, 2000, 34, 3907-3916.
11. R. R. Navarro, K. Sumi, N. Fujii and M. Matsumura, *Water Research*, 1996, 30, 2488-2494.
12. S. Kagaya, H. Miyazaki, M. Ito, K. Tohda and T. Kanbara, *Journal of hazardous materials*, 2010, 175, 1113-1115.
13. G. Zong, H. Chen, R. Qu, C. Wang and N. Ji, *Journal of hazardous materials*, 2011, 186, 614-621.
14. G. Crini, *Progress in polymer science*, 2005, 30, 38-70.
15. F. Wang and M. Ge, *Textile Research Journal*, 2012, 0040517512454188.
16. H. Tang, C. Chang and L. Zhang, *Chemical Engineering Journal*, 2011, 173, 689-697.
17. G. Z. Kyzas and E. A. Deliyanni, *Molecules*, 2013, 18, 6193-6214.
18. N. Rahbar, A. Jahangiri, S. Boumi and M. J. Khodayar, *Jundishapur journal of natural pharmaceutical products*, 2014, 9.
19. J. D. Merrifield, W. G. Davids, J. D. MacRae and A. Amirbahman, *Water research*, 2004, 38, 3132-3138.
20. C. Jeon and K. Ha Park, *Water research*, 2005, 39, 3938-3944.
21. N. Li, R. Bai and C. Liu, *Langmuir*, 2005, 21, 11780-11787.
22. S. R. Dhakate, A. Gupta, A. Chaudhari, J. Tawale and R. B. Mathur, *Synthetic Metals*, 2011, 161, 411-419.
23. N. Fiol and I. Villaescusa, *Environmental Chemistry Letters*, 2009, 7, 79-84.
24. N. Singh, T. Ahuja, V. N. Ojha, D. Soni, S. S. Tripathy and I. Leito, *SpringerPlus*, 2013, 2, 453.
25. N. Singh and A. Sarkar, *ASIAN JOURNAL OF CHEMISTRY*, 2003, 15, 1593-1597.

RSC Advances Accepted Manuscript

26. S. Saber-Samandari and M. Gazi, *Separation Science and Technology*, 2013, 48, 1382-1390.
27. M. Rinaudo, G. Pavlov and J. Desbrieres, *Polymer*, 1999, 40, 7029-7032.
28. K. Sun and Z. Li, *Express Polymer Letters*, 2011, 5, 342-361.
29. S. Tripathi, G. Mehrotra and P. Dutta, *International Journal of Biological Macromolecules*, 2009, 45, 372-376.
30. U. K. Parida, A. K. Nayak, B. K. Binhani and P. Nayak, *Journal of Biomaterials and Nanobiotechnology*, 2011, 2, 414.
31. A. Pawlak and M. Mucha, *Thermochimica acta*, 2003, 396, 153-166.
32. C. Yuwei and W. Jianlong, *Chemical Engineering Journal*, 2011, 168, 286-292.
33. L. Jin and R. Bai, *Langmuir*, 2002, 18, 9765-9770.
34. K. Vimala, M. M. Yallapu, K. Varaprasad, N. N. Reddy, S. Ravindra, N. S. Naidu and K. M. Raju, *Journal of Biomaterials and Nanobiotechnology*, 2011, 2, 55.
35. Y.-T. Jia, J. Gong, X.-H. Gu, H.-Y. Kim, J. Dong and X.-Y. Shen, *Carbohydrate Polymers*, 2007, 67, 403-409.
36. K. Nakane, T. Yamashita, K. Iwakura and F. Suzuki, *Journal of Applied Polymer Science*, 1999, 74, 133-138.
37. K. Lisha, S. M. Maliyekkal and T. Pradeep, *Chemical Engineering Journal*, 2010, 160, 432-439.
38. H. Cui, Y. Qian, Q. Li, Q. Zhang and J. Zhai, *Chemical Engineering Journal*, 2012, 211, 216-223.
39. B. Chen, Z. Zhu, J. Ma, Y. Qiu and J. Chen, *J. Mater. Chem. A*, 2013, 1, 11355-11367.
40. P. K. Tripathi, M. Liu, Y. Zhao, X. Ma, L. Gan, O. Noonan and C. Yu, *Journal of Materials Chemistry A*, 2014, 2, 8534-8544.
41. L. W. Low, T. T. Teng, A. Ahmad, N. Morad and Y. S. Wong, *Water, Air, & Soil Pollution*, 2011, 218, 293-306.
42. Y.-S. Ho and G. McKay, *Chemical Engineering Journal*, 1998, 70, 115-124.
43. M. I. El-Khaiary, G. F. Malash and Y.-S. Ho, *Desalination*, 2010, 257, 93-101.
44. H. Ghoveisi, J. Farhoudi, M. Omid and A. M. Mazdeh, 2011.
45. A. M. Donia, A. A. Atia and K. Z. Elwakeel, *Journal of hazardous materials*, 2008, 151, 372-379.

RSC Advances Accepted Manuscript

46. L. Dambies, C. Guimon, S. Yiacoumi and E. Guibal, *Colloids and Surfaces A: Physicochemical and Engineering Aspects*, 2000, 177, 203-214.
47. L. Zhou, Z. Liu, J. Liu and Q. Huang, *Desalination*, 2010, 258, 41-47.
48. C. Karthika and M. Sekar, *Res. J. Environment. Sci*, 2012, 1, 34-41.
49. I. Langmuir, *Journal of the American Chemical society*, 1918, 40, 1361-1403.
50. P. K. Tripathi, M. Liu and L. Gan, *RSC Advances*, 2014, 4, 23853-23860.

RSC Advances Accepted Manuscript

Figure caption:

Fig.1: SEM and EDAX of composites nanofibers **(a)** Before adsorption (**b)** After adsorption of Hg (II)

Fig. 2: Elemental (C, O, N, Ce & Hg) mapping Ce-PVA-CHT composite nanofibers after Hg (II) adsorption

Fig.3: FTIR of a) PVA-CHT, b) PVA-CHT with Ce and c) Composite nanofibers after Hg (II) adsorption

Fig. 4: XRD of Ce-PVA-CHT composite nanofibers (a) before and (b) after adsorption of Hg (II)

Fig. 5: XPS of Ce-PVA-CHT composite nanofibers before and after adsorption of Hg (II)

Fig. 6: (a) Effect of contact time on adsorption capacity (q_e) of Hg (II), (b) Pseudo second order Kinetics

Fig.7: Pseudo first order kinetics

Fig. 8: (a) pH_{pzc} (b) Effect of pH, (c) Effect of dose and (d) Effect of Ce content in PVA-CHT

Fig. 9: (a) Effect of initial concentration of Hg (II) on adsorption and (b) Langmuir adsorption Isotherm

Fig. 10: Freundlich Isotherms

RSC Advances Accepted Manuscript